

Structural Defect(s) in $\text{CaCu}_{3+x}\text{Ti}_4\text{O}_{12+\delta}$ Solid Solution Estimated via Reitveld Refinement Method

Mohamad Johari ABU^{1,a}, Mohd Fadzil AIN^{2,b}, Julie Juliewatty MOHAMED^{3,c}, and Zainal Arifin AHMAD^{1,d*}

¹Structural Materials Niche Area, School of Materials and Mineral Resources Engineering, Universiti Sains Malaysia, Engineering Campus, 14300 NibongTebal, Penang, Malaysia.

²School of Electrical and Electronic Engineering, Universiti Sains Malaysia, Engineering Campus, 14300 NibongTebal, Penang, Malaysia.

³Faculty of Bioengineering and Technology, Universiti Malaysia Kelantan, Jeli Campus, Locked Bag No. 100, 17600 Jeli, Kelantan, Malaysia.

^amjohari87@yahoo.com, ^beemfadzil@usm.my, ^cjuliewatty.m@umk.edu.my, ^{d*}srzainal@usm.my

ABSTRACT. The structural defect(s) in $\text{CaCu}_{3+x}\text{Ti}_4\text{O}_{12+\delta}$ ($-0.02 \leq x \leq 0.02$) solid solution prepared by conventional solid-state reaction method was comprehensively investigated. X-ray diffraction (XRD) pattern of the materials exposed that a monophasic CCTO without any traces of secondary phase was presented in all samples. Refinement analysis on the structure of solid solution exposed that the crystallite size and strain as determined by Scherrer's equation and Reitveld method is not matched to each other. However, further refinement analysis exposed that the Reitveld method is more reliable to elucidate the structure of solid solution since it has more broadening parameters (e.g. particle, instrument, etc.) than that of Scherrer's equation. The possible mechanism of the solid solution formation was studied by correlating the lattice parameter and bonds length to the several defects and compensation mechanisms of oxygen/cation vacancy and cation disorder substitution. The change of bond length (Δd) with variation of x was evaluated, and the result showed that the Ti-O (6x) and Cu-O (4x) bond for Cu-deficient sample ($x < 0$) have the smallest Δd value as compared to other bonds due to Coulombic attraction between affective charge carrier of ($\text{TiO}_5\text{V}_o^\bullet$ and $\text{TiO}_5\text{V}_o^{\bullet\bullet}$) and (CuO_4' and TiO_6'). Similarly, the smallest Δd value in the Cu-excess sample ($x > 0$) has been correlated due to Coulombic attraction of TiO_6' and $(\text{Cu}_{\text{Ti}})''\text{O}_5\text{V}_o^{\bullet\bullet}$.

Keywords: CCTO, Nonstoichiometry, Structural defect, Reitveld refinement;

Received: 15.10.2017, **Revised:** 15.12.2017, **Accepted:** 30.02.2018, and **Online:** 20.03.2018;

DOI: 10.30967/ijcrset.1.S1.2018.429-434

Selection and/or Peer-review under responsibility of Advanced Materials Characterization Techniques (AMCT 2017), Malaysia.

1. INTRODUCTION

$\text{CaCu}_3\text{Ti}_4\text{O}_{12}$ (CCTO) perovskite-like ceramic oxide has received considerable attentions in recent years due to its colossal relative dielectric constant (ϵ_r) up to 10^5 , which is nearly constant over a wide range of frequencies (static field dc - 1 MHz) and temperatures (100 - 600 K), without undergoing any ferroelectric phase transition [1]. Such properties are essential to allow smaller capacitive components, which offers an opportunity to reduce the dimension of microelectronic devices. Unfortunately, the loss tangent ($\tan\delta$) of CCTO was still too large (0.05 - 0.2 at 1 kHz), its breakdown field was just at 2 kV/cm and even shows non-Ohmic properties similarly to the ZnO varistor [2], but still not fit in the standard of a relaxor either, thus has become the roadblock for many technical applications.

Besides the application of views, the colossal dielectric constant of CCTO also have attracted attentions for researchers to clarify the main origin of this phenomenon. So far, the internal barrier layer capacitor (IBLC) model of Schottky-type potential barriers arising from n-type semiconducting grains and insulating interfaces as been widely accepted [3,4]. The real origin mechanism responsible for the electrical heterogeneity between grain and grain boundary has been explained related to the nonstoichiometry oxygen and cations, even though the starting reactant was prepared in a perfect stoichiometry formulation of CCTO. Models based on oxygenloss [5], cation reduction/oxidation [6] and cation deficiency/excess [7] are reported responsible for semiconductivity of grain, while the accumulation of defects such as twin boundaries, dislocation and stacking faults in the intergranular regions of grain boundary is responsible for insulating property.

The oxygen loss mechanism (e.g. $\text{O}_\delta^- \rightarrow \text{V}_\text{O}^{\bullet\bullet} + 2e^- + \frac{1}{2}\text{O}_2 \uparrow$) is commonly observed for many perovskite-based titanates when heated at $>1000^\circ\text{C}$ and/or in reducing atmosphere [5] and the formation of oxygen vacancy and free electron. The compensation occurs by partial reduction of Ti^{4+} into Ti^{3+} (or TiO_6') to preserve the local electro neutrality. On the other hand, Cu vacancy and segregation are commonly observed in the CCTO ceramic prepared by solid-state reaction due to the diffusion distance of atoms is longer than wet-chemistry methods. Based on this fact, three mechanisms were proposed namely (1) Cu deficiency mechanism relates to the formation of Cu vacancy during heating and the compensation occurs via partial reduction of neighbour Cu^{2+} into Cu^+ (or CuO_4') and partial occupation of Ti^{4+} into Cu site [8], (2) Cu segregation mechanism only valid for CCTO ceramic heated at $>1025^\circ\text{C}$ lead to Cu moved outward from the perovskite structure and the formation of Cu vacancy. Compensation occurs via partial oxidation of Cu^{2+} to Cu^{3+} [9] and (3) Cu excess mechanism is responsible for the formation of vacancies at Ti and O sites, whose compensated by partial occupation Cu at Ti site (or $(\text{Cu}_{\text{Ti}})''\text{O}_5\text{V}_\text{O}^{\bullet\bullet}$) and the formation of O vacancy [9]. Besides that, the last mechanism is proposed due to limited diffusion of oxygen at grain boundary during the cooling stage, which prevent reoxidation of Cu^+ into Cu^{2+} [10], while the compensation is possibly by partial reduction of Ti^{4+} into Ti^{3+} . The presence of compensating ions e.g. Cu^+ , Cu^{3+} and Ti^{3+} is recorded by XPS analysis [9,11], Cu loss detected by EDX analysis [9] and cation disorder is proposed by first principle calculation methods [12]. However, the detection of those structural defects via XRD analysis is scarcely reported in literatures, while the estimation study to relate structural defects formation to the certain ion(s) and its bond length still not been attempted.

To best of our reviews and knowledges, it is actually possible to detect some structural defects in CCTO ceramic through the details examination of crystal structure. The presence of extra local-charges due to defects and compensation mechanisms at the certain ions would increase the contraction force of cation-oxygen and cation-cation, hence slightly reducing the bond length or vice versa. Therefore, in this work, Cu nonstoichiometry CCTO ceramic samples were prepared via conventional solid-state reaction method. The possible defects formation in the CCTO perovskite was investigated via Reitveld refinement method.

2. MATERIALS AND METHODS

The CCTO samples were prepared via SSR method from commercial starting raw materials of CaCO_3 (purity $>99\%$, Sigma-Aldrich), CuO (purity $>99\%$, Sigma-Aldrich) and TiO_2 (purity $>99.9\%$, Merck). Appropriate amounts of powder were prepared according to the various stoichiometry ratios of $\text{CaCu}_{3+x}\text{Ti}_4\text{O}_{12+\delta}$ ($x = -0.02, -0.01, 0, 0.01$ and 0.02), which further designed as SCu-2, SCu-1, SCu0, SCu+1 and SCu+2, respectively. All powder ratios were dry-mixed separately using a rotary mill machine with zirconia ball as grinding media and deionized water as solution media at a constant speed of 150 rpm for 24 hours. Afterwards the mixed powders were calcined in air at 900°C for 12 hours. The degranulation powder was adopted manually by agate mortar and pestle, before being compacted into a green body (rectangular) form ($14 \times 14 \times 4 \text{ mm}^2$) and then sintered in air at 1040°C for 10 hours with a constant heating and cooling rate of $5^\circ\text{C}/\text{min}$. The phase composition and structure of all samples were recorded using an X-ray diffractometer (D8 Advance, Bruker-AXS) with Ni-filtered $\text{CuK}\alpha_1$ ($\lambda = 1.54056 \text{ \AA}$) radiation in a wide range 2θ of $10 - 90^\circ$.

The phase identification and composition of obtained XRD profiles were determined by PANalytical X'Pert High score (Plus) 3.0 software (Reitveld refinement method - automatic mode). Priors to structure calculation, the details of peaks profile e.g. position (θ), intensity (I), d-spacing (d) and full-width at half maximum (FWHM) or peak width (β) was determined by fitting technique (automatic - default), then the lattice parameter (a) was calculated according to Eq. 1.

$$a = d_{(hkl)} \sqrt{h^2 + k^2 + l^2} \quad (1)$$

Meanwhile, the crystallite size (L_c) and strain (ϵ) of CCTO were calculated using Scherrer's equation (using single-line peak width of (220) plane: designed as L_{CS} and ϵ_s , respectively) and Reitveld refinement method (using full-pattern integral breadth: designed as L_{CR} and ϵ_R , respectively). The fully crystalline NIST 660a SRM LaB_6 standard material with β equal to 0.087° was used as the instrument broadening affects. The bond length (d) of cation-oxygen/cation was computed directly from the software after the refinement process is completed. Noted that the refinement steps of structure determination were followed well-known Rietveld's refinement strategy.

3. RESULTS AND DISCUSSION

Fig. 1 shows XRD pattern for cubic CCTO perovskite (SCu0) and solid solutions and their Reitveld refinement results are further listed in Table 1. Apparently, all diffraction peaks could be fully indexed to all planes of body-centered cubic perovskite-related structure under $Im\bar{3}$ (No. 204) space group, agrees well with those reported in Inorganic Crystal Structure Database (ICSD file no. 96-100-8181). No extra peaks associated to the secondary phase or contaminations has been observed, indicated that the variation of x value for both system (deficiency and excess) is under solubility limits of Cu atom in CCTO lattice structure. However, it is worth to mention that the absence of diffraction peaks for the secondary phase does not mean that the excess of CuO is avoided as an amorphous impurity phase in the intergranular regions of grain boundaries. In addition, at low content (below 2-3%), the Cu-related impurity phase may not be able to be detected by XRD machine due to its detection accuracy. The convergence was achieved for most samples, where the agreement indices for three reliabilities of residual (R_p , R_{exp} and R_{wp}) and GoF value are less than 10% and in the range of 1-2, respectively.

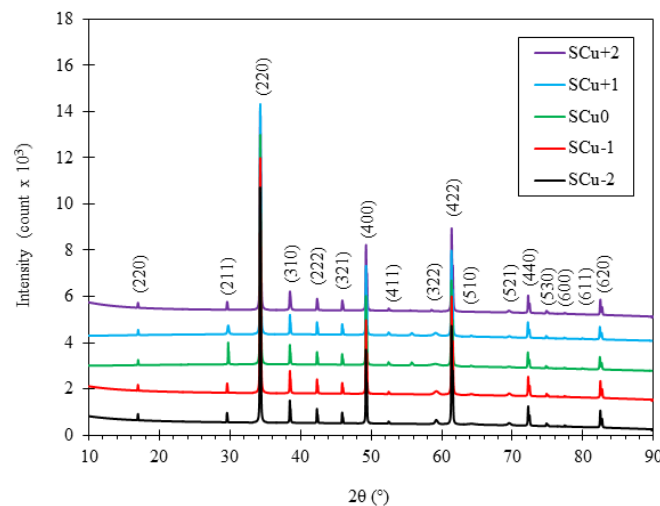


Fig. 1 XRD pattern of $\text{CaCu}_{3+x}\text{Ti}_4\text{O}_{12+\delta}$ ceramics sintered at 1040°C for 10 hours in air

Further interpretation of the peak profiles indicated that the CuO composition (x) has strong effects to the crystallite size and strain, lattice parameter and bonds length. Noted that the crystallite size and strain were

determined by Scherrer's equation and Reitveld method, in order to make clear distinctive of broadening parameters involved: Scherrer's (refined only instrumental and particle size, while the others e.g. size + microstrain + temperature + solid solution inhomogeneity are not involved) and Reitveld method (all factors above are refined except solid solution inhomogeneity).

Table 1 Reitveld refinement results of cubic CCTO perovskite and $\text{CaCu}_{3+x}\text{Ti}_4\text{O}_{12+\delta}$ solid solution

Properties		Sample					
		SCu-2	SCu-1	SCu0	SCu+1	SCu+2	
CCTO	$Y_{(220)}(^{\circ})$	34.2971(4)	34.3062(4)	34.3099(9)	34.2942(4)	34.2853(5)	
	$I_{(220)}$ (Count)	9448(81)	9445(82)	9688(65)	9107(82)	7537(67)	
	$\beta_{(220)}(^{\circ})$	0.099(1)	0.100(1)	0.106(3)	0.096(1)	0.122(1)	
	$d_{(220)}(\text{\AA})$	2.61251	2.61184	2.61157	2.61272	2.61338	
	Scherrer	$L_{CS}(\text{\AA})$	7236	6680	4570	Maximum	2481
		$\epsilon_S(\%)$	0.067	0.070	0.086	0.057	0.121
	Reitveld	$L_{CR}(\text{\AA})$	Maximum	Maximum	Maximum	Maximum	2047
		$\epsilon_R(\%)$	0.029	0.031	0.037	0.036	0.038
	$a(\text{\AA})$	Ca-Ca (6x)	7.38929	7.38740	7.38664	7.38989	7.39175
		Ca-O (12x)	2.60405(2)	2.60339(2)	2.60311(5)	2.60426(2)	2.60492(1)
	Bond length (\AA)	Ca-Ti (8x)	3.19966(2)	3.19884(2)	3.19850(5)	3.19992(2)	3.20072(1)
		Cu-O (4x ₁)	1.96049(1)	1.95999(1)	1.95979(3)	1.96065(2)	1.96115(1)
		Cu-O (4x ₂)	2.78246(2)	2.78175(2)	2.78146(5)	2.78269(3)	2.78339(2)
		Cu-O (4x ₃)	3.26797(2)	3.26714(2)	3.26679(6)	3.26824(3)	3.26906(2)
		Cu-Ti (8x)	3.19966(2)	3.19884(2)	3.19850(5)	3.19992(2)	3.20072(1)
		Ti-O (6x)	1.96189(2)	1.96138(2)	1.96118(4)	1.96205(2)	1.96254(1)
		O-O (1x ₁)	2.63945(2)	2.63878(2)	2.63850(6)	2.63967(3)	2.64033(2)
		O-O (1x ₂)	2.89956(3)	2.89882(3)	2.89851(7)	2.89980(3)	2.90053(2)
		O-O (4x ₁)	2.76351(2)	2.76280(2)	2.76251(5)	2.76373(2)	2.76443(1)
		O-O (4x ₂)	2.78550(2)	2.78479(2)	2.78449(5)	2.78573(3)	2.78643(2)
Agreement Indices	Residual (%)	R_p	2.07102	2.01541	2.73154	2.82596	1.73432
		R_{exp}	4.63535	4.54480	4.74822	5.85630	3.78061
		R_{wp}	7.55384	7.54799	5.87419	8.22005	7.60132
	GoF	1.62962	1.66080	1.23714	1.40363	2.01061	

*Noted that the maximum value for L_{CS} and L_{CR} that could be calculated via Scherrer's equation and Reitveld method is $\geq 10000 \text{\AA}$ and 27913.4\AA , respectively

The results showed that the crystallite size and strain obtained from those methods are not matched to each other, except SCu+2 sample shows comparable L_c value, conveying that the standard broadening parameters using Scherrer's equation seems not appropriate to elucidate the effects of solid solution. Therefore, further clarification of lattice structure by using Reitveld method only will be taken into accounts. As seen from Table 1, the crystallite size of all samples is comparable to each other (27913.4\AA), except SCu+2 sample shows smaller size (2047\AA). Interestingly, the lattice strain has changed linearly with the variation of

x; where the highest ϵ_R value is recorded for the SCu+2 sample, which is consistent to the previous literature's propositions of (1) partial substitution of bigger Cu^{2+} ($\sim 0.62 \text{ \AA}$) ions into Ti^{4+} ($\sim 0.605 \text{ \AA}$) site [8] and (2) partial reduction of Ti^{4+} to Ti^{3+} ($\sim 0.67 \text{ \AA}$) ions [5], hence affects the size broadening related to solid solution. Besides that, the lattice parameter of CCTO is increased proportionally with the increase or decrease of x value. This relationship is actually following the defects and compensation mechanisms as proposed from many literatures [5-12]. The deficiency of CuO could promote the formation of V_{Cu} and V_{O} . Compensations occur via partial reduction of Cu^{2+} into Cu^+ (0.77 \AA) and partial occupation of Ti^{4+} into V_{Cu} site, hence increase the lattice parameter. With continuous increase in lattice parameter with decreasing of x value proof that the compensating Cu^+ ions is dominated. In contrast, the excess of CuO in CCTO would lead to the formation of (i) V_{Ti} and V_{O} within crystal structure and (ii) Cu segregation produces V_{Cu} at the face-centered of crystalline. Compensation occurs via (partial occupation of Cu^{2+} into V_{Ti} site and partial reduction of Ti^{4+} to Ti^{3+}) and partial oxidation of Cu^{2+} to Cu^{3+} ($\sim 0.64 \text{ \AA}$), respectively. The continuous increasing of a value with the increase of x is only preserve for the domination of compensating Ti^{3+} and Cu^{3+} ions, whilst the Cu_{Ti} can be ignored because it's has an opposite effect.

To support numerous defect mechanisms above, the change of bond length ($\Delta d = d_i - d_o$; where d_i and d_o are bond length of solid solution and cubic CCTO perovskite, respectively) was used to illustrate the effect of CuO variation (Fig. 2). It is clearly seen that the bond length increases monotonically with the increase/decrease of x value. Among them, only Cu-O ($4x_1$) and Ti-O ($6x$) bonds displayed a lowest change, while Ca-Ti ($8x$), Cu-O ($4x_3$) and Cu-Ti ($8x$) bonds considerably displayed the highest change. Both Cu-O ($4x_1$) and ($4x_3$) bonds are located at face-centred positions of the cubic perovskite (Fig. 2b), but shows not comparable in Δd value, implying that the defect clusters with different of charges would be introduced in the ceramics. In principle, the detection of oxygen vacancy at faced centered ($\text{TiO}_5\text{V}_o^\bullet$ and $\text{TiO}_5\text{V}_o^{\bullet\bullet}$) and corner ($\text{CaO}_{11}\text{V}_o^\bullet$ and $\text{CaO}_{11}\text{V}_o^{\bullet\bullet}$) of cubic perovskite structure has been proposed by Oliveira et al. [13]. For Cu deficient sample, both $\text{TiO}_5\text{V}_o^\bullet$ and $\text{TiO}_5\text{V}_o^{\bullet\bullet}$ defects could attracted to CuO_4' and TiO_6' (due to limited oxygen content), thus reducing the Ti-O ($6x$) and Cu-O ($4x_1$) bond length. However, the lowest change of Ti-O ($6x$) and Cu-O ($4x_1$) bonds for Cu excess CCTO is associated to the presence of TiO_6' and $(\text{Cu}_{\text{Ti}})''\text{O}_5\text{V}_o^{\bullet\bullet}$.

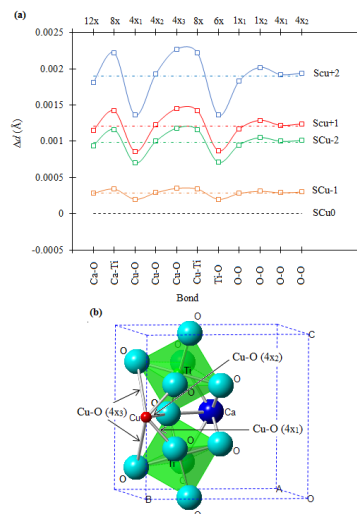


Fig2 (a) Change of bonds length for CCTO ceramic with variation of Cu content (noted that the dash-line across each line is representing the average value) and (b) Schematic diagram of partial CCTO perovskite representing the location of Cu-O bond.

4. SUMMARY

The structural defect(s) in $\text{CaCu}_{3+x}\text{Ti}_4\text{O}_{12+\delta}$ ($x = -0.02, -0.01, 0, 0.01$ and 0.02) solid solution prepared by conventional solid-state method was investigated via Reitveld refinement method. A monophasic CCTO without any traces of secondary phase was observed for all prepared samples. The first distinctive of crystallite size and strain by using Scherrer's equation and Reitveld method revealed that they are generated the different values, probably due to the different of computing data (peak width and integral breath) applied, but further analysis exposed that the Reitveld method is more suitable to elucidate the effects of Cu nonstoichiometry because its refined more broadening effects than that of Scherrer's equation. The possible formation of structural defects in CCTO ceramic was studied by correlated the present result (e.g. crystallite size and strain, lattice parameter and bonds length) to the previous defects and compensation mechanisms as proposed in the literatures. The results show that the variation of CuO composition has a great influence to the lattice structure of CCTO by creating a substantial amount of defects with different in charges.

ACKNOWLEDGEMENT

This work was financially supported by the Fundamental Research Grant Scheme (FRGS) of Malaysia under grant number of 6071263 and 000284. Also, the authors greatly acknowledges to the Ministry of Higher Education of Malaysia for awarding MyBrain15 – (MyPhD).

REFERENCES

- [1] C.C. Homes, T. Vogt, S.M. Shapiro, S. Wakimoto, A.P. Ramirez, Optical Response of High Dielectric Constant Perovskite-Related Oxide, *Science*, 293 (2001) 673-676.
- [2] X.T. Zhao, R.J. Liao, N.C. Liang, L.J. Yang, J. Li, J.Y. Li, Role of Defects in Determining the Electrical Properties of ZnO Ceramics, *J. Appl. Phys.*, 116 (2014) 014103.
- [3] R. Schmidt, M.C. Stennett, N.C. Hyatt, J. Pokorny, J. Prado-Gonjal, M. Li, D.C. Sinclair, Effects of sintering temperature on the internal barrier layer capacitor (IBLC) structure in $\text{CaCu}_3\text{Ti}_4\text{O}_{12}$ (CCTO) ceramics, *J. Eur. Ceram. Soc.*, 32 (2012) 3313-3323.
- [4] M.J. Abu, J.J. Mohamed, M.F. Ain, Z.A. Ahmad, Phase structure, microstructure and broadband dielectric response of Cu nonstoichiometry $\text{CaCu}_3\text{Ti}_4\text{O}_{12}$ ceramic, *J. Alloys and Comp.*, 683 (2016) 579-589.
- [5] D.F.K. Hennings, Dielectric materials for sintering in reducing atmosphere, *J. Eur. Ceram. Soc.*, 21 (2013) 1637-1642.
- [6] R. Schmidt, S. Pandey, P. Fiorenza, D.C. Sinclair, Non-stoichiometry in " $\text{CaCu}_3\text{Ti}_4\text{O}_{12}$ " (CCTO) ceramics, *RSC Adv.*, 3 (2013) 14580-14589.
- [7] J.J. Romero, P. Leret, F. Rubio-Marcos, A. Quesada, J.F. Fernandez, Evolution of the intergranular phase during sintering of $\text{CaCu}_3\text{Ti}_4\text{O}_{12}$ ceramics, *J. Eur. Ceram. Soc.*, 30 (2010) 737-742.
- [8] M. Li, A. Feteira, D.C. Sinclair, A.R. West, Influence of Mn doping on the semiconducting properties of $\text{CaCu}_3\text{Ti}_4\text{O}_{12}$ ceramics, *Appl. Phys. Lett.*, 88 (2006) 232903.
- [9] T.T. Fang, L.T. Mei, H.F. Ho, Effects of Cu stoichiometry on the microstructures, barrier-layer structures, electrical conduction, dielectric responses, and stability of $\text{CaCu}_3\text{Ti}_4\text{O}_{12}$, *Acta Mater.*, 54 (2006) 2867-2875.
- [10] C.C. Wang, L.W. Zhang, Oxygen-vacancy-related dielectric anomaly in $\text{CaCu}_3\text{Ti}_4\text{O}_{12}$: post-sintering annealing studies, *Phys. Rev. B*, 74 (2006) 024106-024112.
- [11] L. Zhang, Z.J. Tang, Polaron relaxation and variable-range-hopping conductivity in the giant-dielectric-constant material $\text{CaCu}_3\text{Ti}_4\text{O}_{12}$, *Phys. Rev. B*, 70 (2004) 174306-174312.
- [12] P. Delugas, P. Alippi, V. Fiorentini, V. Raineri, Reorientable dipolar CuCa antisite and anomalous screening in $\text{CaCu}_3\text{Ti}_4\text{O}_{12}$, *Phys. Rev. B*, 81 (2010) 0811041-0811044.
- [13] L.H. Oliveira, E.C. Paris, W. Avansi, M.A. Ramirez, V.R. Mastelaro, E. Longo, J.A. Varela, Correlation Between Photoluminescence and Structural Defects in $\text{Ca}_{1+x}\text{Cu}_{3-x}\text{Ti}_4\text{O}_{12}$ Systems, *J. Am. Ceram. Soc.*, 96 (2013) 209-217.